

Quasi-biennial Modulation of Planetary-Wave Fluxes in the Northern Hemisphere Winter

TIMOTHY J. DUNKERTON AND MARK P. BALDWIN

Northwest Research Associates, Inc., Bellevue, Washington

(Manuscript received 22 May 1990, in final form 10 October 1990)

ABSTRACT

Using 25 years of National Meteorological Center (NMC) data for 1964–88 the relation between tropical and extratropical quasi-biennial oscillations (QBOs) was examined for zonally averaged quantities and planetary-wave Eliassen–Palm fluxes in the Northern Hemisphere winter. The extratropical QBO discussed by Holton and Tan existed in both temporal halves of the dataset. Autocorrelation analysis demonstrated that it was an important mode of interannual variability in the extratropical winter stratosphere. Correlation with the tropics was strongest when 40-mb equatorial winds were used to define the tropical QBO. Easterly phase at 40 mb implied a weaker than normal polar night jet and warmer than normal polar temperature and vice versa. An opposite relationship was obtained using 10-mb equatorial winds. The association between tropical and extratropical QBOs was observed in about 90% of the winters and was statistically significant.

It is shown that planetary-wave Eliassen–Palm fluxes were generally consistent with the extratropical QBO. These fluxes were more (less) convergent in the midlatitude (subtropical) upper stratosphere in the 40-mb east (= easterly) phase category relative to the west category. The composite difference in flux divergence was a dipole, the location of which coincided with the observed mean zonal wind anomaly. The difference was strongest in early- to midwinter. However, composites of planetary-wave life cycles were similar in the two phase categories, with only slightly more events, slightly larger events, and larger mean flow response in the east category. There was very good correlation between planetary-wave flux convergence and observed mean flow tendencies on a daily basis, but the tendencies were smaller in magnitude.

1. Introduction

It is well known that there is large interannual variability in the Northern Hemisphere winter stratosphere. The greatest variation is due to stratospheric sudden warmings (Scherhag 1952; Labitzke 1977, 1981, 1982; Schoeberl 1978; Quiroz 1986) that are associated with the anomalous growth, upward propagation, and breaking of planetary Rossby waves (Matsuno 1971; McIntyre 1982; Andrews et al. 1987). Major warmings as defined by WMO criteria¹ have occurred in about half of the observed winters (1955,² 1957, 1958, 1963, 1966, 1968, 1970, 1971, 1973, 1977, 1979, 1981, 1984, 1985, 1987, 1988, and 1989). They are commonly spaced about two years apart; on this account it was suggested that their timing may be influenced by the quasi-biennial oscillation of the equatorial lower stratosphere (Labitzke 1982; McIntyre 1982). Labitzke

noted that more major warmings occurred in the 50-mb QBO east phase (namely 8 in 13 years, compared to 4 in 16 years for the west phase). Subsequently Labitzke and van Loon (1988) uncovered a remarkable correlation between North Pole temperatures and centimetric solar flux when the data are partitioned according to the phase of the QBO at 45 mb. It was previously noted that major warmings occurred in the west phase near solar maxima (Labitzke 1982, 1987). There is no known physical mechanism underlying the apparent solar/QBO/weather relationship (Geller 1989) and there is some question whether the solar cycle interpretation is unique (Baldwin and Dunkerton 1989a) or stable (Hamilton 1990). Pursuing a different line of thought, Dunkerton et al. (1988) noted that major warmings have not occurred in the “deep westerly” phase of the QBO, in agreement with a suggestion by McIntyre (1982) that planetary waves responsible for the warming are likely to be sensitive to winds in a deep tropical layer. This association suffered a setback in December 1987 when a major warming occurred in the deep westerly phase (Baldwin and Dunkerton 1989b). Summarizing this evidence it is clear that the stratospheric sudden warming is an important component of interannual variability, but an association with the tropical QBO is imperfect and unlikely to entirely explain the occurrence of “major” warmings.

¹ A major warming requires that the 10-mb mean temperature at the North Pole exceed that at 60°N and the mean zonal wind reverse to easterly as far south as this latitude.

² The convention here is that the “1955” northern winter is actually 1954/55, and so on.

Corresponding author address: Dr. Timothy J. Dunkerton, Northwest Research Associates, P.O. Box 3027, Bellevue, WA 98009.

Part of the problem could be due to the WMO definition of a major warming. This definition is useful in describing the dynamical phenomenon, i.e., the rapid distortion, erosion, and/or splitting of the main circumpolar vortex (McIntyre and Palmer 1983, 1984; Dunkerton and Delisi 1986; Baldwin and Holton 1988). However, when it comes to interannual variability, the question is not simply whether a major warming occurred in a particular winter. There are additional factors that determine how much a particular warming contributes to interannual variation. First, there is the *timing* of the warming, whether in early, middle, or late winter. Very early or very late warmings generally have little effect on the average midwinter circulation and temperature. Second, there is the *persistence* of warming, or duration of anomaly once the criteria are met. Similarly, any *precursors* or *preconditioning* before a major warming will contribute to the duration of an anomaly. In general, major warmings have precursors and some persistent effect; their contribution to interannual variation depends on timing.

A broader definition of the "anomaly" contributing to interannual variation is any perturbation of large size and long duration relative to climatology (e.g., Dole 1983). Such anomalies in the winter stratosphere are usually associated with major warmings or planetary-wave events that fall short of the WMO criteria. They are remarkably large and persistent in comparison to tropospheric standards and contain a large zonally symmetric component. The nature of these anomalies can be appreciated by examining polar temperature time series in Naujokat et al. (1988) based on Berlin data. For comparison, we derived these series using NMC data (1964–88) and found similar results when averaged over the entire polar cap inside of 72°N , as shown in Fig. 1. The climatological 50-mb temperature declines to a minimum in late December and rises thereafter. Observed temperatures oscillated about climatology with a typical peak-to-peak amplitude of 10–40 K and time scale of 20–50 days or more. Anomalies were therefore of long duration with respect to a sudden warming (major warmings are indicated by asterisks in Fig. 1). (This was consistent with precursors and persistent elevation of temperature following the warming.) At the same time, anomalies were of short duration with respect to the entire winter. That is, most winters contained both anomalously warm and cold periods. In any winter, then, there was cancellation between anomalies. Incidentally, it is noted that those winters containing a major warming in December through February often had colder temperatures than normal in March–April and vice versa. This may be due to the fact that the climatological average included major warmings in most months, but in any given year there was at most one or two warmings. A "cold" anomaly may indicate the absence of a major warming.

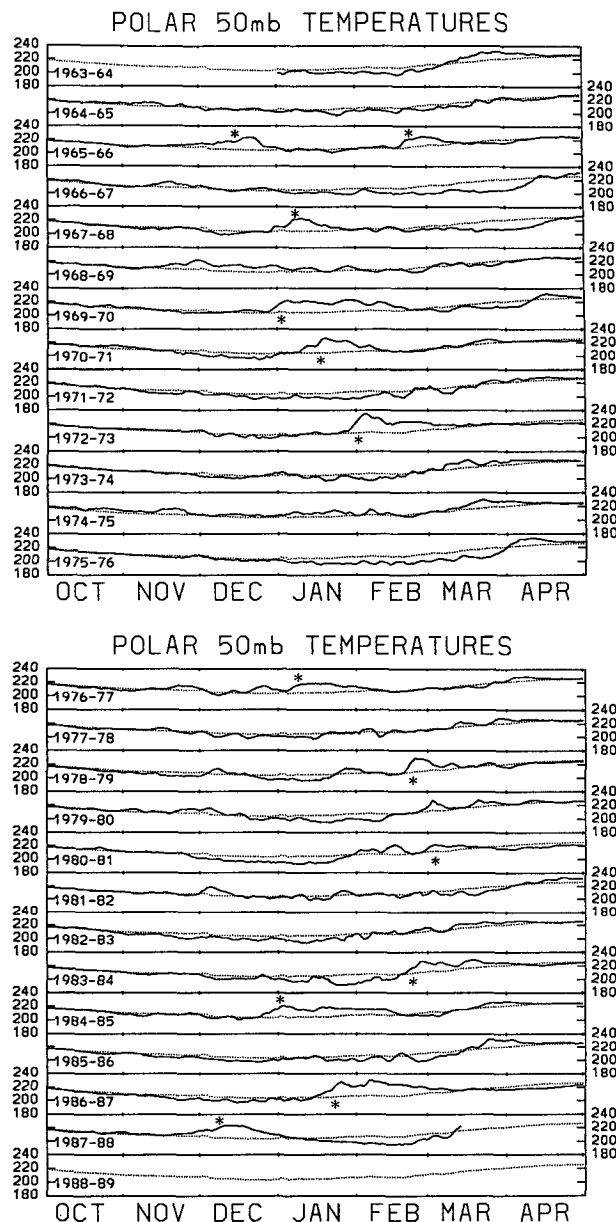


FIG. 1. Average temperature (K) north of 72°N at the 50-mb level. Climatological average shown as dotted line. Asterisks denote major warmings.

This persistent aspect of interannual variability is well known in the literature, and individual winter months, or seasons, were described as disturbed or "relatively undisturbed, cold," recognizing the persistence (e.g., Labitzke 1981). The axisymmetric component of the anomaly was noted by Quiroz (1981) who found a seesaw pattern in zonal mean wind between individual winters. In some winters the polar night jet was anomalously strong and vice versa. By thermal wind balance, this alternate strengthening and

weakening of the jet was associated with cooling and warming of the polar stratosphere and a weak opposite tendency at low latitudes as seen in 1-point correlation maps (Baldwin and Dunkerton 1989a). That is not to say that the pattern was exactly axisymmetric since planetary waves 1 and 2 were also associated with warm and cold winters, respectively (Labitzke 1981).

Not surprisingly, this component of interannual variability became associated with the tropical QBO. Holton and Tan (1980) noted that the 50-mb QBO west phase coincided rather well with anomalous strengthening of the polar night jet and a modest attenuation of the tropospheric jet stream. An opposite anomaly was observed in the east phase. Those authors also found differences in stationary planetary wave structure associated with the zonally symmetric oscillation. However, an attempt by Holton and Tan (1982) to discover differences in Eliassen–Palm flux between the two QBO phases was inconclusive. Adding to their dilemma was a suggestion by van Loon et al. (1982) that the El Niño–Southern Oscillation might explain the polar oscillation (Wallace and Chang 1982; Holton 1983). Van Loon and Labitzke (1987) attempted to separate QBO and ENSO signals, but the question is not yet resolved.³ However, it is clear that by using a quantitative statistic (e.g., strength of the jet) rather than a logical criterion (e.g., WMO definition), Holton and Tan obtained better evidence for a tropical–extratropical QBO connection than that based on “major warmings” per se. This improvement, as we shall see, is due largely to the timing of major warmings and their effect on average circulation statistics.

At this point, two kinds of question arise. First, is the extratropical QBO still related to the tropical QBO, dynamically or otherwise, and is this relationship more significant in some months than in others? Which levels of the tropical QBO are most important? Second, independent of the tropical QBO, can we discover a relationship between planetary-wave fluxes and the extratropical oscillation?

With regard to the first question, we find that the Holton–Tan relationship remains valid in the more recent data, an impressive record when compared to other examples from meteorology. Statistical significance, however, depends on the stringency of statistical tests. Tests demanding a certain autocorrelation in random time series yield a lower significance than those that do not, although in both cases the level of significance is high. The persistence of tropical–extratropical

relationship, correct in about 90% of the winters in our 25-yr sample, seems remarkable. The same could be said about the shorter data record of the Southern Hemisphere and an apparent effect of the tropical QBO on Antarctic ozone depletion (Bojkov 1986; Garcia and Solomon 1987; Lait et al. 1989; Kerr 1989).

With regard to the second question, the results indicate a fairly close relationship between planetary-wave fluxes and the zonal mean circulation, particularly when transient contributions to the flux are retained, all zonal wavenumbers are included, and the analysis extended to the upper stratosphere where composite differences in EP flux are largest. This result provides no independent verification of a connection to the tropical QBO (as one would not expect waves and mean flow to be independent), but it reinforces a belief that planetary Rossby wave transport is the most important effect governing the circulation of the northern winter stratosphere.

In section 2, the data source and processing methods are described, and the relation between major warmings and persistent anomalies is examined. Significance of the tropical–extratropical QBO connection is also discussed, as this result underlies the following presentation (in section 3) of composite differences in mean circulation between east and west phases. Section 4 contains an analysis that is independent of the tropical QBO: we discuss the teleconnectivity and spatial autocorrelation of the zonally averaged circulation. Section 5 presents composite differences in Eliassen–Palm cross sections thought to be associated with the zonal mean variations. Consistent with previous studies of extratropical circulation, the wave forcing significantly exceeds the observed response of the mean flow, suggesting—in this context—that planetary-wave fluxes are an important part of the extratropical oscillation.

2. Data analysis and overview

a. Dataset and analysis methods

The dataset used in this study are National Meteorological Center (NMC) heights and temperatures at 1200 UTC from 1000 to 10 mb for the period 1 January 1964–23 October 1978 and from 1000 to 1 mb for the period 24 October 1978–12 March 1988. Winds at all levels were calculated by the linear balance method (Robinson 1986; Hitchman et al. 1987; Randel 1987a); the zonally averaged component was obtained from gradient balance. NMC analyses were interpolated to a 4° lat \times 5° long grid, and spherical harmonic smoothing with triangular truncation at wavenumber 15 was applied to the data above 100 mb in the manner described by Baldwin and Dunkerton (1989b). Computation of Eliassen–Palm flux used the quasi-geostrophic form [Eqs. (2.2a, b) of Dunkerton et al. 1981]

³ Their ENSO cold event composite continued mostly QBO west category years, while warm events were distributed more or less equally between the two phase categories. This explains part of their ENSO composite difference, but does not explain an anomaly in the warm event category per se. In any case, the sample size was small, and the issue is not likely to be resolved without a longer data record and further theoretical study.

but with horizontal perturbation winds derived from linear balance. For other details of the analysis method see Baldwin and Dunkerton (1989b).

b. Correlation of tropical and extratropical QBO

As noted by Holton and Tan (1980, 1982) the east phase of the tropical QBO near 50 mb is associated with weaker winds in the polar night jet and vice versa. Their analysis extended from 1962–77 using the NMC data up to 10 mb; our result, for the longer time period 1964–88 as shown in Fig. 2, confirms their discovery. We found optimum correlation between 10-mb winds at 62°N and the tropical QBO when the equatorial wind at 40 mb was used. The equatorial wind was obtained from Singapore (1.3°N) and was not deseasonalized. As shown later, results using 30- or 50-mb equatorial wind were similar, but produced slightly lower correlations. In Fig. 2, wind components were normalized by their standard deviation and the average was removed, indicating a normalized anomaly. The two time series are correlated with coefficient = 0.64. This figure shows the average winds for December, January, and February (DJF). As discussed later, comparably good results were obtained in any of the individual months November through February.

Figure 2 is the best result, or nearly so, and indicates what could be expected from the tropical–extratropical relationship for the 25-yr Northern Hemisphere record. The correlation was not perfect, but there were only two years (1980 and 1984) when the two anomalies were grossly separated and of opposite sign. In 1982 and 1988, the extratropical anomaly did not cross the axis and achieve the same sign as the Singapore anomaly, but the tendency of the anomaly was correct. In general, the relationship after 1978 was less convincing than that before 1978. This was due mainly to weak variation of the extratropical anomaly in 1980–1984.

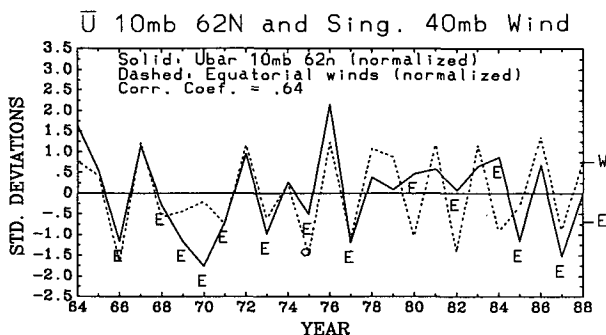


FIG. 2. DJF-average mean zonal wind at 10 mb, 62°N (solid) and Singapore 40-mb wind (dashed). Both quantities were normalized by their standard deviation and the average was removed.

c. Relationship to major warmings

Most, but not all, of the easterly anomalies in Fig. 2 could be attributed to major warmings (1966, 1968, 1970, 1971, 1973, 1977, 1985, and 1987). The major warming of February 1979 occurred too late to affect the DJF anomaly; this anomaly remained positive in accord with the equatorial value. Similarly the March 1981 major warming had no effect. The February 1984 event did not influence the DJF anomaly although, in this case, the equatorial anomaly was of opposite sign. The December 1987 warming occurred too early to affect the DJF value (plotted here at “88”) so the relation to a (westerly) tropical anomaly was maintained. As noted by Baldwin and Dunkerton (1989b) this midwinter period was, in fact, relatively undisturbed.

A few years, such as 1969, 1975, and 1982 (almost), contained easterly anomalies but no major warming. On the whole, then, the relationship between tropical and extratropical wind anomalies was stronger than the relationship with major warmings. This improvement was due either to the timing of major warming (which, if too early or too late, did not affect the DJF average even though the warming occurred in the QBO west phase) or to an easterly anomaly with no major warming. We note, however, that the correlation displayed in Fig. 2 was not perfect; it was grossly incorrect in 2 out of 25 cases and gave exactly the same sign in 21 out of 25 cases. In this respect it seems comparable to the Southern Hemisphere correlation discussed by Lait et al. (1989) (see also Kerr 1989).

d. Statistical significance

While the relation shown in Fig. 2 is not perfect, it would be difficult to obtain by random variations. In order to estimate the statistical significance of the relation seen in Fig. 2, two Monte Carlo simulations were performed. In both tests the time series of extratropical winds was replaced by random numbers. In the first test, it was assumed that in the absence of a relation between the tropical and extratropical winds, the time series of extratropical winds could be replaced by numbers drawn from a normal distribution (random normal deviates). Since each number in the time series is drawn independently of the last, the average autocorrelation of such a time series is zero. This is equivalent to the assumption that in the absence of a QBO–extratropical connection the extratropical circulation would have no memory of the previous winter. When the tropical winds are correlated with random normal deviates, the probability of obtaining a correlation coefficient of at least 0.62 is 0.1%. This relationship is significant at the 1.0% level for any coefficient exceeding 0.47, which, as shown later, includes most of the extratropical stratosphere.

The observed autocorrelation of the time series of extratropical winds at 10 mb, 62°N is -0.24 . In the first Monte Carlo simulation it was assumed that this autocorrelation would have been zero if there were no relation between tropical and extratropical winds. A more stringent test would demand that the random time series have some autocorrelation similar to the observed extratropical anomaly, in other words, that there exists an extratropical QBO unrelated to the tropical QBO (Trenberth 1980). To simulate this possibility we constrained the random time series to have a lag 1 yr autocorrelation in the range -0.20 to -0.28 , centered about the observed autocorrelation -0.24 . In this case the probability of obtaining a correlation of 0.65 is 0.1% . For the same coefficient, at least probabilities are generally about twice as large as in the unconstrained test. In either case, then, the observed correlations have high significance.

This discussion pertains to mean circulation variables (zonal wind, polar temperature, geopotential, etc.) for which the extratropical and tropical QBOs are well correlated. In the next section, composite differences of these fields are shown. Because of hydrostatic and gradient wind balance, these quantities are not independent. Comments about statistical significance pertain to all of these fields alike; the composites add nothing to the significance already determined. It is important to keep this in mind when discussing a perceived relationship between atmospheric variables and external forcing (Livezey and Chen 1983; Baldwin and Dunkerton 1989a).

Later in this paper, composite differences of Eliassen–Palm flux are shown supporting our hypothesis that planetary-wave fluxes are consistent with the observed zonally averaged extratropical QBO. It should be noted that because these quadratic fluxes are noisier, less regular, and not linearly related to the mean fields, the estimated significance is considerably lower. There is consistency between waves and mean flow—more evident in the upper than lower stratosphere—but we do not have the same confidence in this relationship.

3. Extratropical composites based on the equatorial QBO

a. Geopotential

Composites were constructed from DJF mean fields and partitioned according to the phase of the equatorial QBO at 40 mb. Results for geopotential are shown in Fig. 3, including zonal mean and wave components averaged over this 3-month interval. Similar results were obtained at 50 and 10 mb, the former level corresponding to that of Holton and Tan (1980). (We show east minus west, whereas they showed west minus east. A positive anomaly indicates a shallower vortex in the QBO east phase, or easterly mean flow anomaly.)

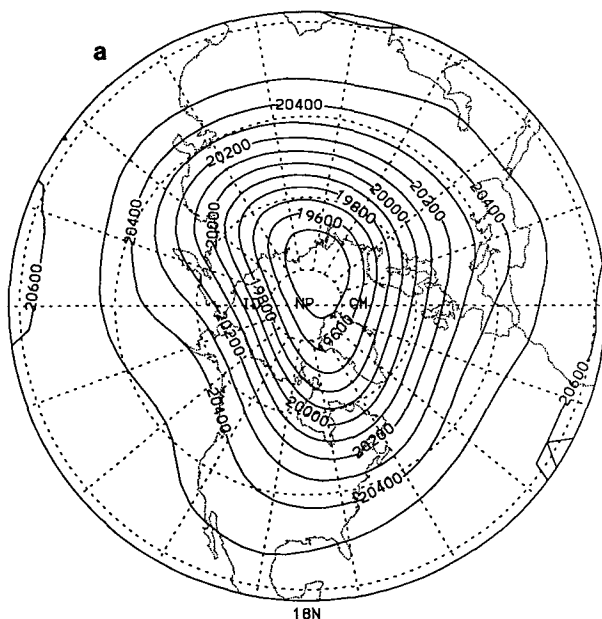
The magnitude of the polar anomaly at 50 mb was a little over 300 gpm, comparable to what Holton and Tan (1980) obtained for December and January. The 10-mb anomaly was twice as large, comparable to that of Holton and Tan (1982) for January–March (JFM). South of about 55°N the anomaly reversed sign; at 50 mb it was rather small (less than 100 gpm). In Holton and Tan (1980) the midlatitude anomalies were larger but appeared at different longitudes in each month. At 10 mb (Fig. 3f) the midlatitude anomaly covered much of the Pacific but was smaller than the corresponding JFM anomaly in Holton and Tan (1982). Figure 3 suggests, then, that the composite difference originated mainly in the depth of the polar vortex, with only a small depression of geopotential surface in midlatitudes. This result differs from Holton and Tan (1980, 1982) and may be due to the more recent years. Figures 4a,b compare the composite difference obtained with data from 1964–75 and 1976–88, respectively. Figure 4a better resembles Fig. 1 of Holton and Tan (1982) than Fig. 4b. Weakening of the composite in Fig. 4b is consistent with the time series of Fig. 2. The phase of the anomaly also changed somewhat.

b. Mean zonal wind

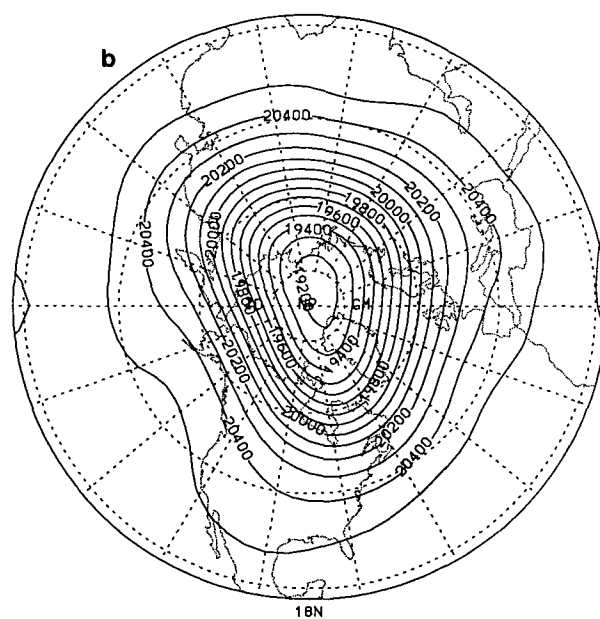
Figure 5 shows the east-minus-west composite difference of DJF mean zonal wind partitioned according to the phase of the equatorial QBO at different levels. All patterns displayed a dipole changing sign around 40°–45°N. Separate calculations (not shown) indicated that the angular momentum anomaly associated with this dipole was nearly *antisymmetric*, such that the amount of angular momentum associated with the polar jet anomaly was comparable but opposite to that contained in the subtropical anomaly.

The 40-mb QBO level generated the largest anomaly and most significant correlation between tropical and extratropical QBOs. Using the 10-mb QBO level, the anomalies reversed sign consistent with phase descent in the equatorial QBO. In other words, the east phase at 10 mb was associated with a *positive* anomaly in the polar night jet. It is the *west* phase at 10 mb that was associated with a negative anomaly in the jet or, more precisely, a *west-over-east* alignment of the equatorial QBO. This would be consistent with the numerical results of Dameris and Ebel (1990). However, it points to a basic ambiguity in the effect of the QBO, namely, whether this effect—if real—originates in the lower stratosphere (such that the east phase reduces the polar night jet) or in the middle stratosphere (such that the west phase reduces the polar night jet). In the first case, diminution of the jet could be associated with a contraction of the waveguide for quasi-stationary waves and possible nonlinear reflection from the critical layer (McIntyre 1982; Killworth and McIntyre 1985). In the second case, planetary-wave amplification might

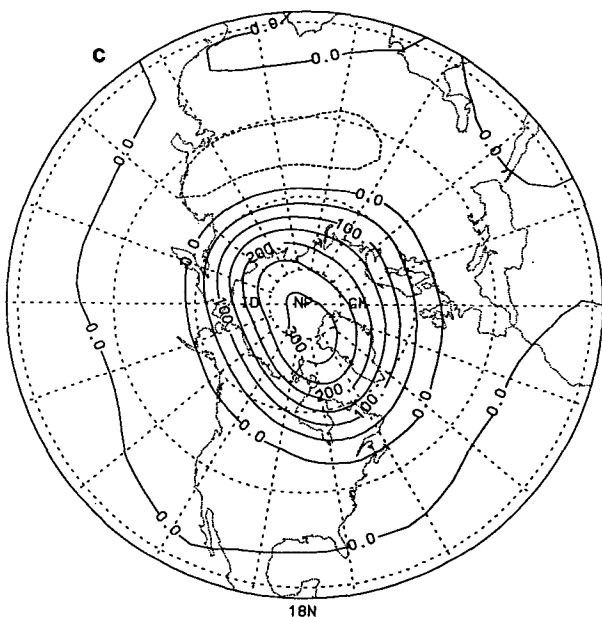
50mb Z: East 40mb QBO. DJF



50mb Z: West 40mb QBO. DJF



50mb Z: E-W 40mb QBO. DJF



10mb Z: East 40mb QBO. DJF

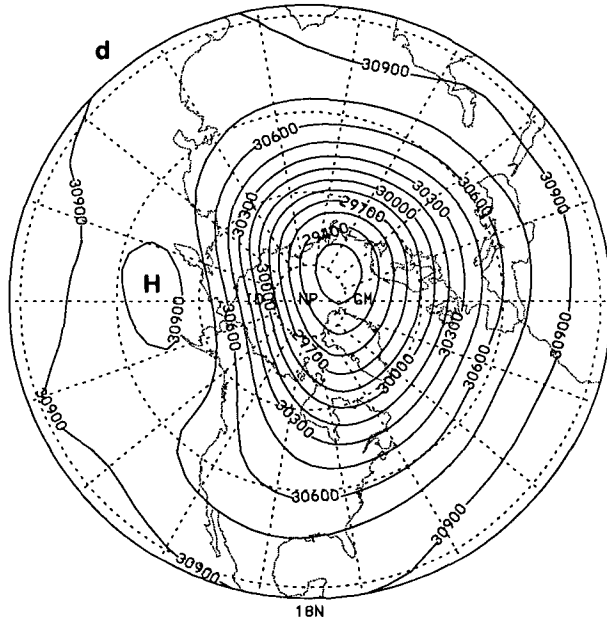


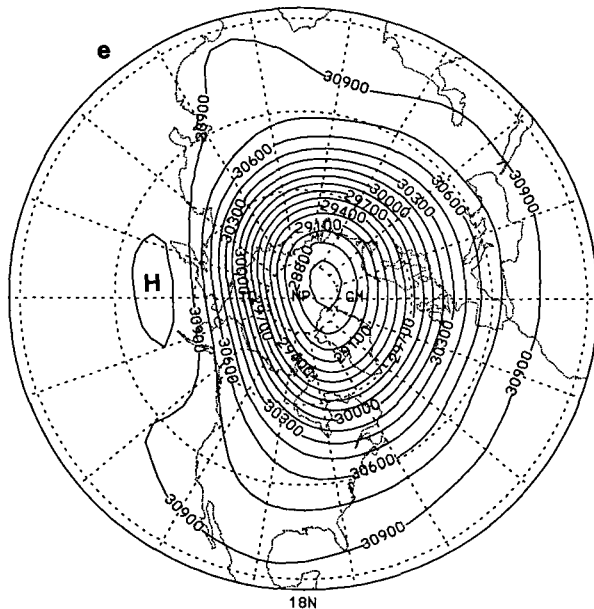
FIG. 3. Geopotential at 50 mb (a-c) and 10 mb (d-f) for Singapore 40-mb QBO east category (a, d), west category (b, e), and composite difference (c, f). (Units: gpm.)

originate from an expanded waveguide in the QBO west phase (i.e., less absorption) or linear reflection from the northern flank of equatorial westerlies [e.g., as implied by Hamilton (1984) and Dunkerton and Delisi (1985)]. This ambiguity cannot be resolved from the data and provides strong justification for numerical studies. In any case, it seems unlikely that a single layer

of the equatorial QBO, such as 40 mb, could influence the entire extratropical atmosphere.⁴

⁴ Using a three-dimensional model D. O'Sullivan (personal communication) obtained a dipole in mean zonal wind similar to ours, due entirely to an easterly anomaly in the equatorial lower stratosphere.

10mb Z: West 40mb QBO. DJF



10mb Z: E-W 40mb QBO. DJF

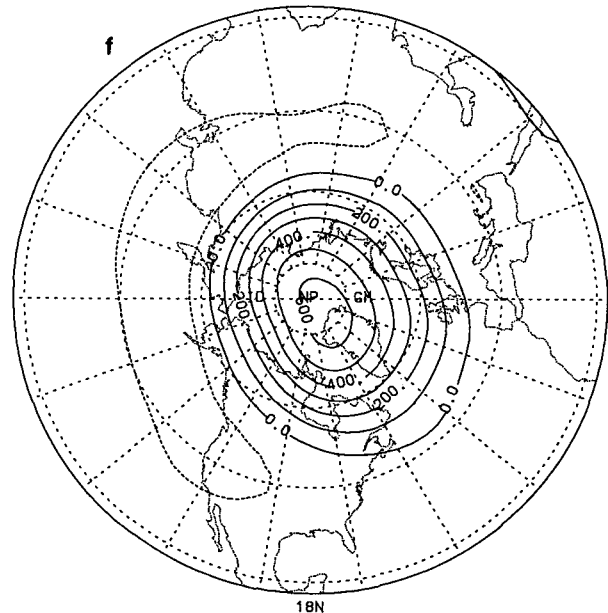
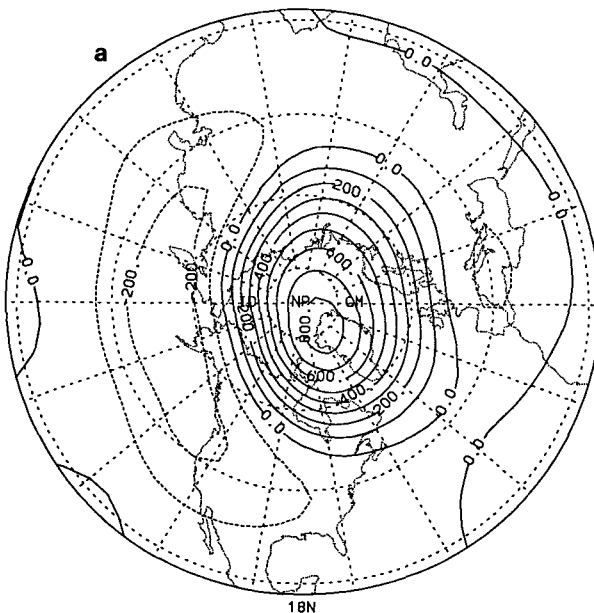


FIG. 3. (Continued)

From Fig. 5b it is apparent that the extratropical QBO penetrated the troposphere. This is consistent with Quiroz (1980) and Holton and Tan (1982), although in our case strengthening of the tropospheric jet stream in the east phase was small relative to the

subtropical anomaly at higher levels. In all cases the polar anomaly penetrated the troposphere with larger amplitude. Spatial autocorrelations discussed in the next section suggest that the subtropical tropospheric and stratospheric anomalies are distinct.

1964-75 10mb Z: E-W 40mb QBO



1976-88 10mb Z: E-W 40mb QBO

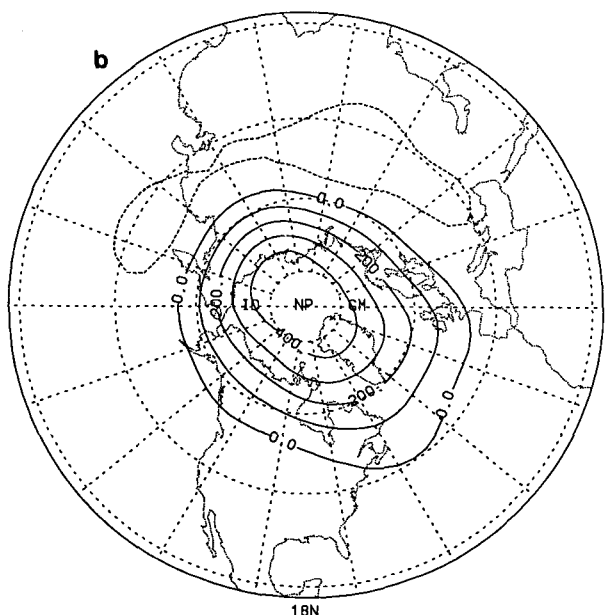


FIG. 4. Geopotential composite difference at 10 mb as in Fig. 2f but for (a) 1964-75 and (b) 1976-88.

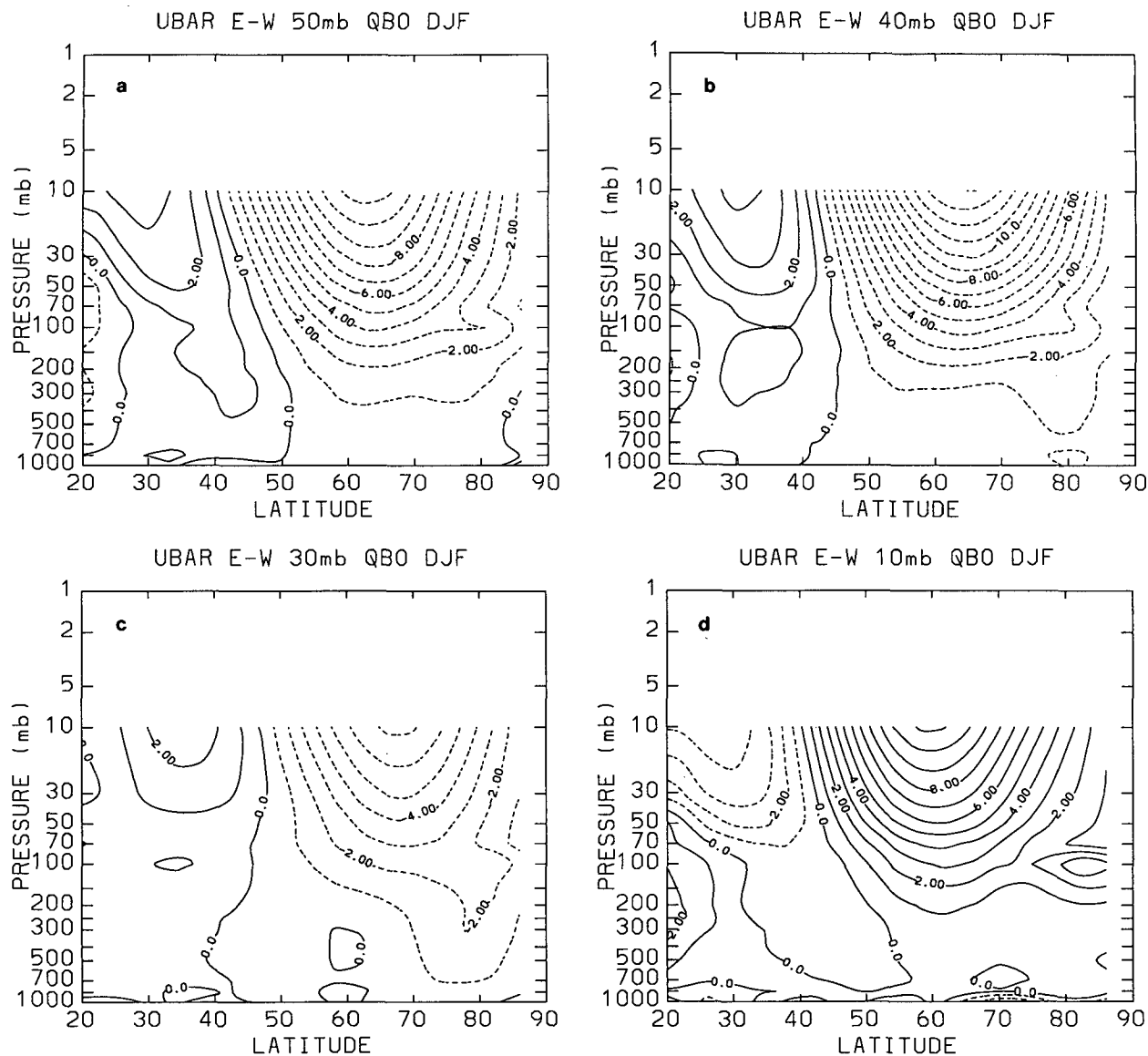


FIG. 5. Composite (east minus west) of DJF mean zonal wind with respect to QBO phase category at (a) 50 mb, (b) 40 mb, (c) 30 mb, (d) 10 mb. (Units: m s^{-1} .)

For the last 10 years (1979–88), the composite difference was smaller in magnitude but similar in structure (Fig. 6). The negative anomaly reached a maximum at 5 or 2 mb, while the positive anomaly in the subtropics peaked near 10 mb before turning equatorward at higher levels. Figure 6, if combined with tropical wind data, would show a westerly QBO anomaly overlying an easterly anomaly at the equator, while in the subtropics the westerly anomaly would slope polewards and downwards before giving way to a distinct easterly anomaly in mid- and high latitudes.

c. Temperature

Composites of DJF temperature difference (east minus west phase) are shown in Figs. 7a,b for 25- and

10-yr records, respectively. The longer record produced a stronger positive anomaly in polar latitudes, consistent with previous discussion. The last 10 years (1979–88) revealed a quadrupole pattern with reversed anomalies in the upper stratosphere, consistent with a maximum wind anomaly in the 5–2 mb layer (Fig. 6).

d. Tropical–extratropical correlations

Figure 2 showed the correlation between DJF Singapore 40-mb wind and NMC mean zonal wind at 10 mb, 62°N . This grid point was selected for its large mean zonal wind anomaly and, as it turns out, had the highest correlation. Coefficients at other grid points are displayed in Fig. 8. Consistent with the anomaly fields (e.g., Fig. 5b), the correlation pattern was a dipole

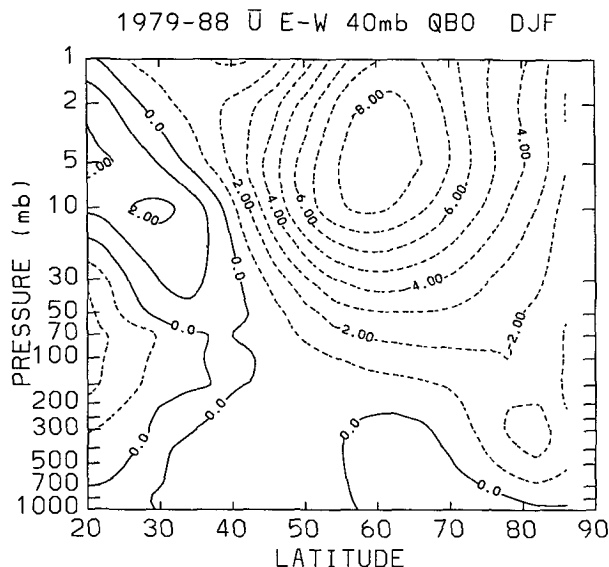


FIG. 6. Composite difference of DJF mean zonal wind as in Fig. 5b, but for 1979–88 only.

changing sign between 40°–45°N. Based on our statistical analysis it appears that the coefficients were highly significant throughout most of the stratosphere and part of the polar upper troposphere. They were less significant in the tropospheric jet stream as noted by Holton and Tan (1982).

Consistent with previous discussion, the correlations were higher in the period 1964–75 than in 1976–88 (Figs. 9a,b respectively). The pattern was robust, nevertheless.

Figure 10 shows a latitude–time view of the correlations between Singapore 40-mb wind and 10-mb NMC winds for successive 3 month periods (JFM,

FMA, . . . DJF). (Values were plotted at the center of each averaging interval so that DJF, for example, appears above “J”). This pattern is very nearly the same as that obtained for individual months, except that December correlations were slightly lower than November’s (not shown). The striking feature of Fig. 10 is a latitudinal shift of the dipole center through the northern winter, beginning near 30°N in October and traveling into polar latitudes by March–April. In general the period November through February had the strongest signal. It was difficult to detect a similar latitudinal shift in the 50-mb maps of Holton and Tan (1980). This effect may be more prominent in the middle stratosphere due to vortex erosion (Butchart and Remsberg 1986).

A separate correlation maximum appeared briefly in northern summer, which we do not understand; it may be a spurious feature due to random correlation.

4. Teleconnectivity and spatial autocorrelations

The material discussed in this section is independent of the tropical QBO and partitioning. It is instructive to look at interannual variability of the extratropical atmosphere apart from the tropical QBO. This analysis revealed that the dipole pattern present in wind anomalies and correlation maps was an important mode of interannual variability in extratropical latitudes.

a. Teleconnectivity

This quantity represents the maximum anticorrelation obtained at a grid point when that point is correlated with all other grid points (in the present case, at lag zero) (e.g., Wallace and Gutzler 1981). Figure 11 shows an example for DJF mean zonal wind. The teleconnectivity was high near 30 mb, 60°N because in this region there was some other grid point where

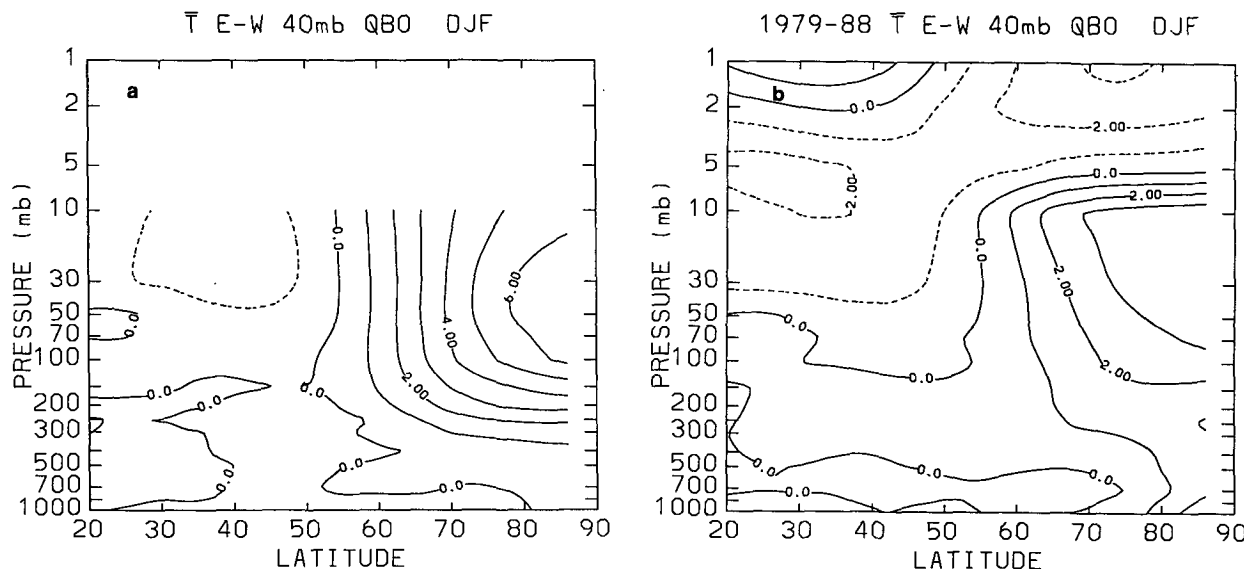


FIG. 7. Composite difference of DJF zonal mean temperature (°C). (a) All years; (b) 1979–88 only.

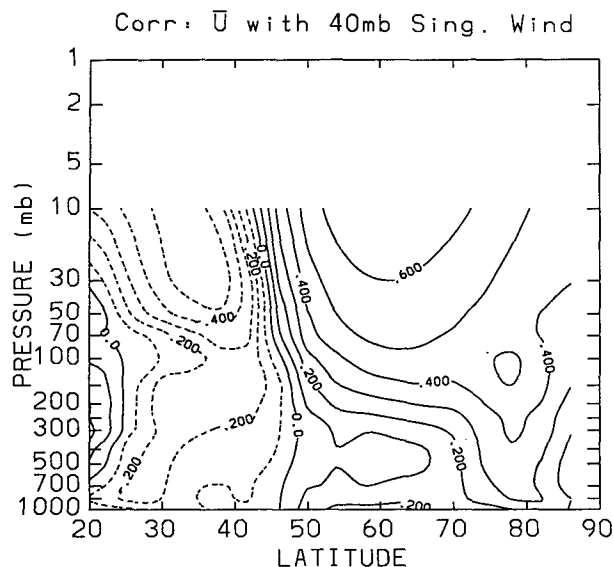


FIG. 8. Correlation between Singapore 40-mb wind and DJF mean zonal wind on the NMC grid.

the zonal wind was anticorrelated with coefficient exceeding -0.85 . The polar atmosphere near 60°N exhibited high teleconnectivity at all levels, whereas in the subtropics there were two distinct centers of action. Details of the teleconnection patterns can be further elucidated by constructing 1-point correlation maps, i.e., the spatial autocorrelations of mean zonal wind at lag zero.

b. Spatial autocorrelations

Figures 12a–d show spatial autocorrelations of DJF mean zonal wind for the 25-yr climatology (i.e., mean zonal wind at a reference gridpoint correlated with mean zonal wind at all other points). Four reference points were chosen from the teleconnectivity diagram in Fig. 11. We refer to these points as “polar stratosphere” (Fig. 12a), “subtropical stratosphere” (Fig. 12b), “polar troposphere” (Fig. 12c), and “subtropical troposphere” (Fig. 12d). All four panels had a similar dipole structure with perfect correlation at the reference grid point and a strong anticorrelation in the opposite half of the dipole (hence, a large teleconnectivity). Correlations decayed vertically away from the reference point, as did anticorrelations. There was a tendency in each diagram for the subtropical correlations to split roughly about the 100-mb level. The polar correlation was uniform by comparison.

Polar stratosphere autocorrelations (Fig. 12a) were similar to the tropical QBO correlation (Fig. 8) but were larger in amplitude, exceeding -0.8 in the opposite half of the dipole. This might suggest that the extratropical oscillation (with lag 1-yr autocorrelation -0.24) existed independently of the tropical QBO; however, it does not explain why the correlation with

the tropical QBO was statistically significant (section 2d). We tentatively conclude that (i) the tropical QBO excited a fundamental, dipole-shaped mode of variability in the extratropical atmosphere, or (ii) apparently by chance the tropical QBO coincided with such a mode of variation for much of the 25-yr record.⁵

Subtropical stratosphere autocorrelations (Fig. 12b) were nearly opposite to those of Fig. 12a. The tropospheric patterns (Figs. 12c,d) were likewise opposite to one another but somewhat narrower than the stratospheric dipole. There was no counterpart of this tropospheric dipole in the tropical QBO correlation (Fig. 8). This fact suggests that while the tropical QBO might have had some effect on the polar troposphere, the tropospheric variability at mid- and subtropical latitudes was of different origin. In any case it was much less correlated with the tropical QBO.

Figure 13 shows the autocorrelation of mean zonal wind for the last 10 years (1979–88) using 10 mb, 62°N as the reference point. This pattern showed a slightly weaker anticorrelation with the subtropical stratosphere and midlatitude troposphere. Also, the correlations decayed with height rather abruptly in the stratosphere.

It should be noted that the subtropical stratospheric anomaly existed in a region of weak mean flow. A 10-yr average DJF mean zonal wind is shown in Fig. 14. The region of weak westerlies is above 100 mb, in the 70–5 mb layer. The subtropical variation was therefore small, but nevertheless well correlated with higher latitudes. As already noted, the two components of angular momentum were comparable in magnitude.

5. Planetary-wave Eliassen–Palm fluxes

a. Composite differences

Composite Eliassen–Palm cross sections for east and west categories (defined using Singapore 40-mb wind) are shown in Figs. 15a,b for the November–December–January average (NDJ). Reasons for choosing this time interval as opposed to DJF are discussed later in this section. The two composites were very similar, showing upward and equatorward refraction of the vectors for both tropospheric synoptic-scale and stratospheric planetary waves, a layer of convergence in the upper troposphere, and smaller convergence in a broad region of the middle stratosphere (Edmon et al. 1980; Dunkerton et al. 1981; Randel, 1987b). Our diagrams compared well to Randel’s, although 25 years of NMC data were used here (Randel used 1979–86).

⁵ A third possibility—that the tropical QBO is somehow influenced by the extratropical QBO—faces several difficulties: e.g., that the tropical QBO is weakly connected to the seasonal cycle (Dunkerton and Delisi 1985; Dunkerton 1990) whereas the extratropical circulation, correlation coefficients, and wave fluxes undergo large seasonal variation in both hemispheres. Vortex erosion during winter contributes to this variation, making it difficult for planetary Rossby wave fluxes to penetrate the equatorial lower stratosphere.

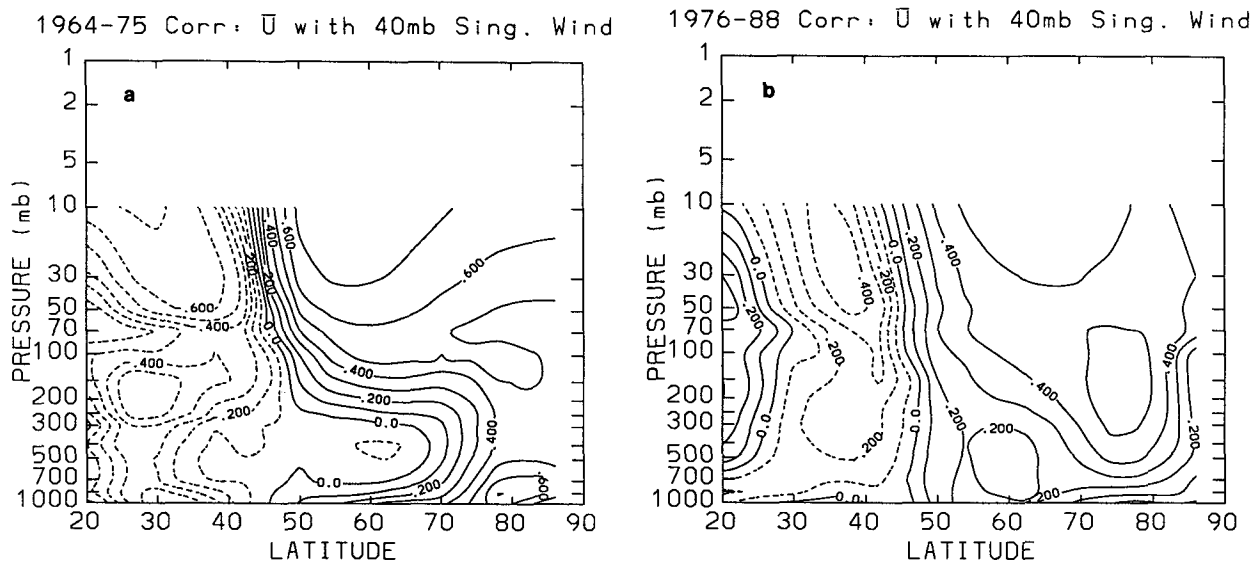


FIG. 9. Correlation as in Fig. 8, but for (a) 1964-75; (b) 1976-88.

The composite difference for NDJ is shown in Fig. 16a. The corresponding plot for DJF was similar (not shown). From this diagram it is clear that while the differences were small relative to Fig. 15, there was stronger stratospheric convergence in the east category and slightly larger upward fluxes. In the upper troposphere there was generally stronger divergence except below 200 mb south of 60°N . In the middle stratosphere, the difference in convergence amounted to about 0.5 to $1.5 \text{ m s}^{-1} \text{ day}^{-1}$. This may not seem large except for the fact that it is a 3-month average and,

were it not for restoring forces, the convergence by itself would produce a zonal wind anomaly of 45 – 135 m s^{-1} . It is an order of magnitude larger than the number quoted by Holton and Tan (1982). (We were puzzled why such a small difference was obtained in their composite.)

For the last ten years (1979–88), the composite difference was similar (Fig. 16b). In the stratosphere there was stronger convergence in midlatitudes and weaker convergence south of 40°N so that the difference composite showed a dipole structure above 50 mb. With

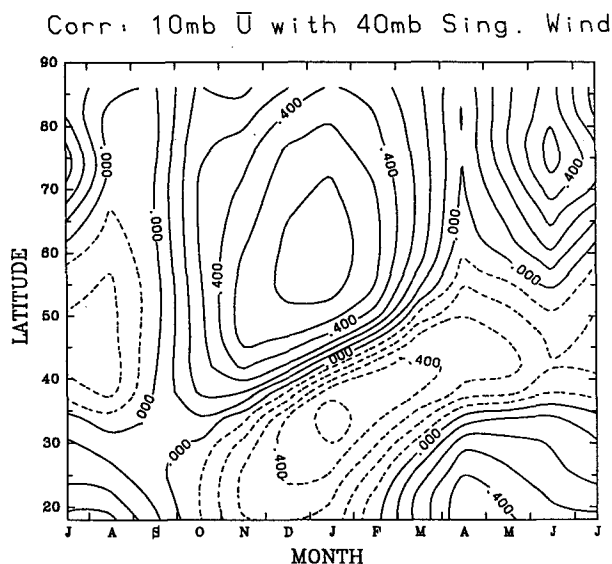


FIG. 10. Latitude-time plot of correlation between Singapore 40-mb wind and NMC 10-mb mean zonal wind, using data averaged in three-month blocks. DJF is plotted above "J," and so on.

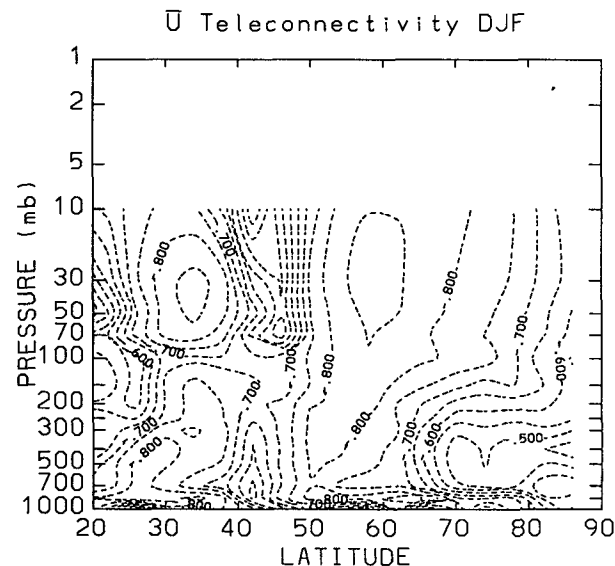


FIG. 11. Teleconnectivity of DJF mean zonal wind with respect to itself. This quantity represents the highest anticorrelation obtained at any grid point when that point is correlated with all other grid points.

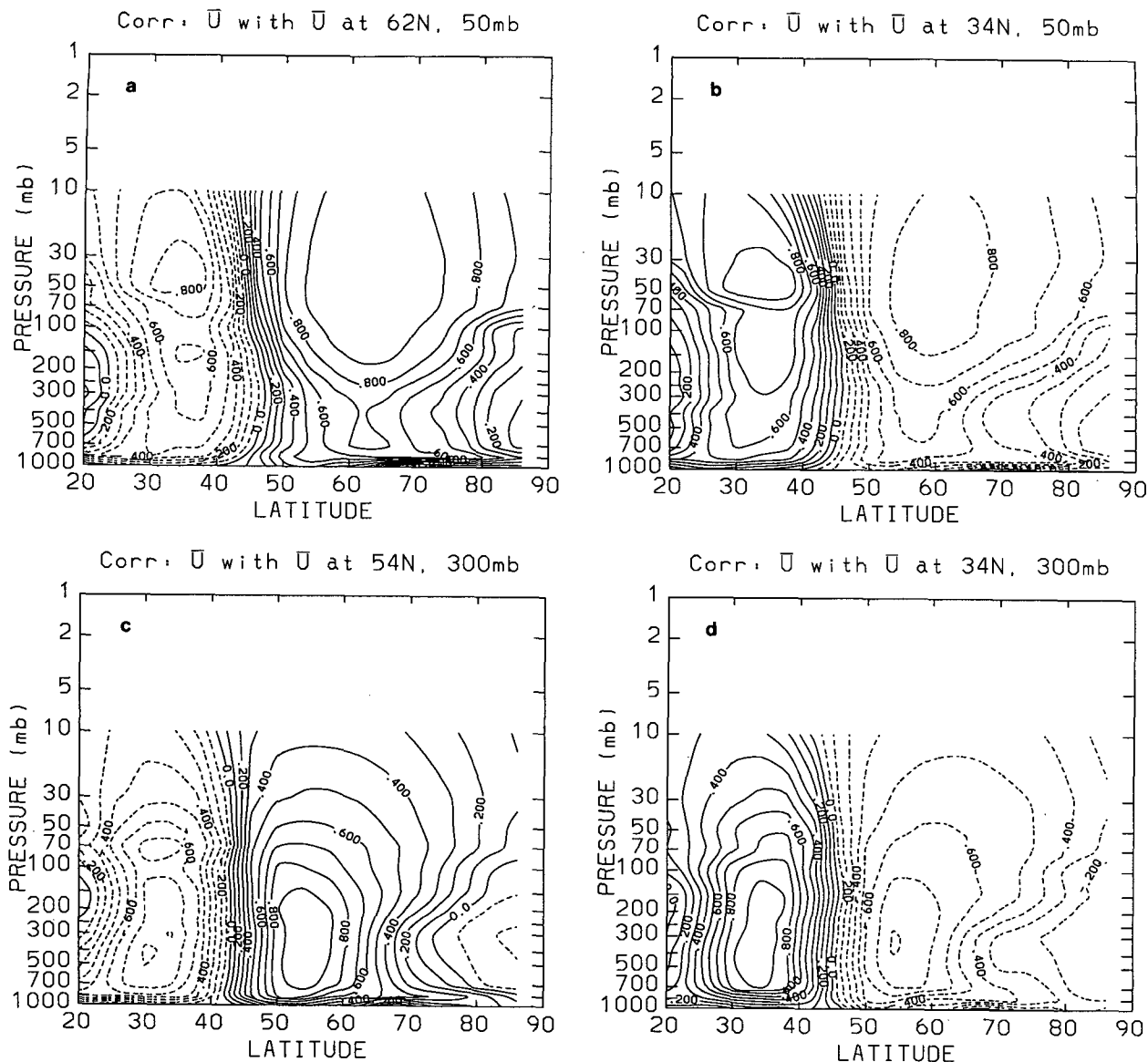


FIG. 12. Spatial autocorrelation of DJF mean zonal wind with reference point at (a) 62°N, 50 mb; (b) 34°N, 50 mb; (c) 54°N, 300 mb; (d) 34°N, 300 mb.

hindsight this feature could be detected in Fig. 16a, although it was mostly present above 10 mb. The divergent half of the dipole did not imply absolute divergence in the east category or in any of the individual years, but less convergence (stronger convergence in the west category). Similarly the poleward tilt of vectors at 2 mb indicated reduced equatorward flux in the east category, not absolute reflection. Our DJF composite had the same features (not shown).

The latitudinal position of the dipole was similar to the mean zonal wind anomaly (Figs. 5b, 6) except at a higher altitude (especially the subtropical part). Vertical spread of the response relative to the

forcing is consistent with the effect of an induced mean meridional circulation (Dunkerton et al. 1981).

While these results partially answer the paradox of Holton and Tan (1982) as far as the *composite* is concerned, the relation between zonally averaged QBO and planetary-wave fluxes is more subtle. It was more difficult to interpret this composite for reasons now discussed.

b. Integrated fluxes and box averages

In order to compress the Eliassen–Palm cross sections into time series form, the flux components, net convergence, and average angular momentum were

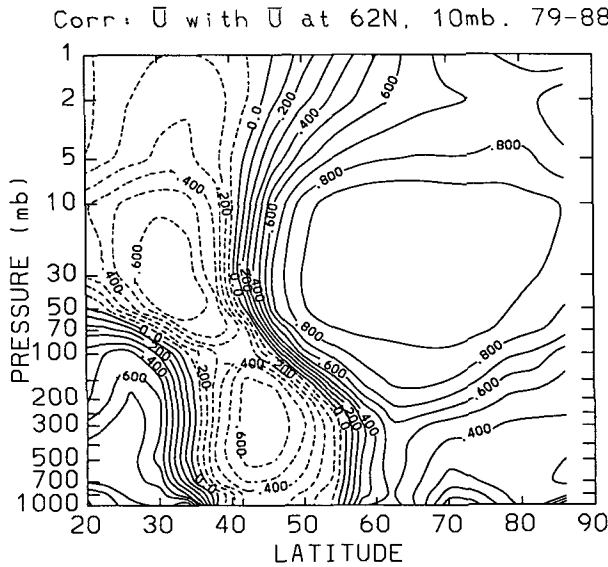


FIG. 13. Spatial autocorrelation of DJF mean zonal wind for 1979-88 only, with reference point at 62°N, 10 mb.

evaluated within two boxes in the latitude-height plane (see Fig. 17). Both boxes extended from 46°N to the pole (corresponding to the polar half of the dipoles shown in Figs. 5b, 16b); the lower box extended vertically from 200 to 10 mb and the upper box from 10 to 1 mb. Data in the upper box were available for ten years only. The mean zonal wind \bar{u} evolves according to

$$\frac{\partial \bar{u}}{\partial t} + \bar{v}^* \left(\frac{1}{a \cos \theta} \frac{\partial}{\partial \theta} \bar{u} \cos \theta - f \right) + \bar{w}^* \bar{u}_z = D_F + \bar{X} \quad (5.1)$$

where \bar{v}^* , \bar{w}^* are meridional and vertical components of the residual mean meridional circulation, f is the Coriolis parameter, D_F is the known Eliassen-Palm flux divergence factor

$$D_F = \frac{\nabla \cdot \mathbf{F}}{\rho_0 a \cos \theta} \quad (5.2)$$

(Dunkerton et al. 1981), and \bar{X} an unknown residual. From (3.1), the angular momentum

$$M = \rho_0 a \cos \theta (\bar{u} + \Omega a \cos \theta), \quad (5.3a)$$

when integrated over part of the latitude-height plane, satisfies

$$\frac{\partial \langle M \rangle}{\partial t} + \dots = F_{\text{NET}} + \langle \bar{X} \rho_0 a \cos \theta \rangle \quad (5.3b)$$

where

$$\langle (\dots) \rangle = \int_{z_1}^{z_2} \int_{46^\circ \text{N}}^{90^\circ \text{N}} (\dots) \rho_0 a \cos \theta d\theta dz, \quad (5.4)$$

$$F_{\text{NET}} = \begin{cases} F_{10} - F_{200} - F_{46^\circ \text{N}}^{(\text{lower})} & \text{in lower box} \\ F_1 - F_{10} - F_{46^\circ \text{N}}^{(\text{upper})} & \text{in upper box} \end{cases} \quad (5.5)$$

$$F_{10} \equiv \int_{46^\circ \text{N}}^{90^\circ \text{N}} F_{(z)} a \cos \theta |_{10 \text{ mb}} d\theta \quad (5.6a)$$

$$F_{200} \equiv \int_{46^\circ \text{N}}^{90^\circ \text{N}} F_{(z)} a \cos \theta |_{200 \text{ mb}} d\theta \quad (5.6b)$$

$$F_{46^\circ \text{N}} \equiv \int_{z_1}^{z_2} F_{(\theta)} \cos \theta |_{46^\circ \text{N}} dz. \quad (5.6c)$$

An example of integrated time series is shown in Figs. 18a,b for lower and upper boxes, respectively, in winter 1983-84. (Note that $F_{46^\circ \text{N}}$ was inverted in this figure and the “net flux” represents convergence, or $-F_{\text{NET}}$.) There was good correlation between the net flux and observed time tendency of integrated angular momentum (in this case, correlation coefficients were 0.71 and 0.80 in lower and upper box respectively). In the lower box the average correlation coefficient for all 25 years was 0.49 with standard deviation 0.16. In the upper box the average correlation was somewhat higher: 0.75 with standard deviation 0.10. In both cases the correlations improved when all resolvable wavenumbers were retained (with triangular truncation at wavenumber 15). Most of the flux in the upper box, however, was due to waves 1 and 2. The highest observed correlation, 0.87, was in the upper box for 1982-83. Agreement between the net flux and observed tendency provided a good check on the numerical calculation and accuracy of the data. It should be kept in mind that the correlation coefficient normalized the data so that any differences in magnitude between the two quantities were ignored. In fact, the observed tendency in angular momentum was only about one-third

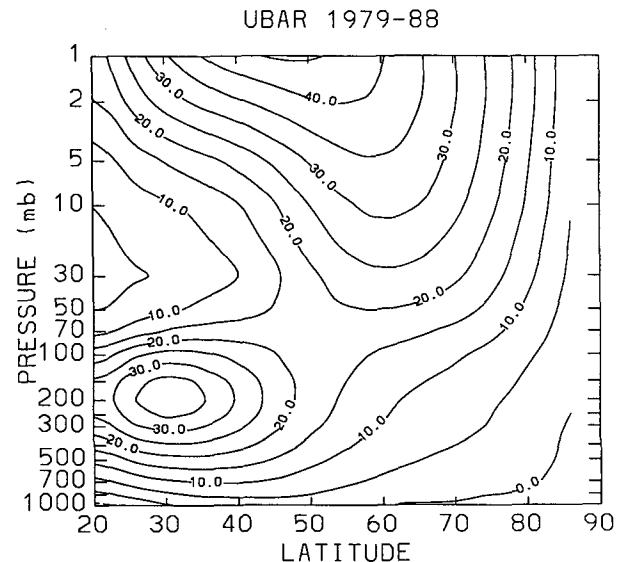


FIG. 14. DJF mean zonal wind for 1979-88. (Units: m s^{-1} .)

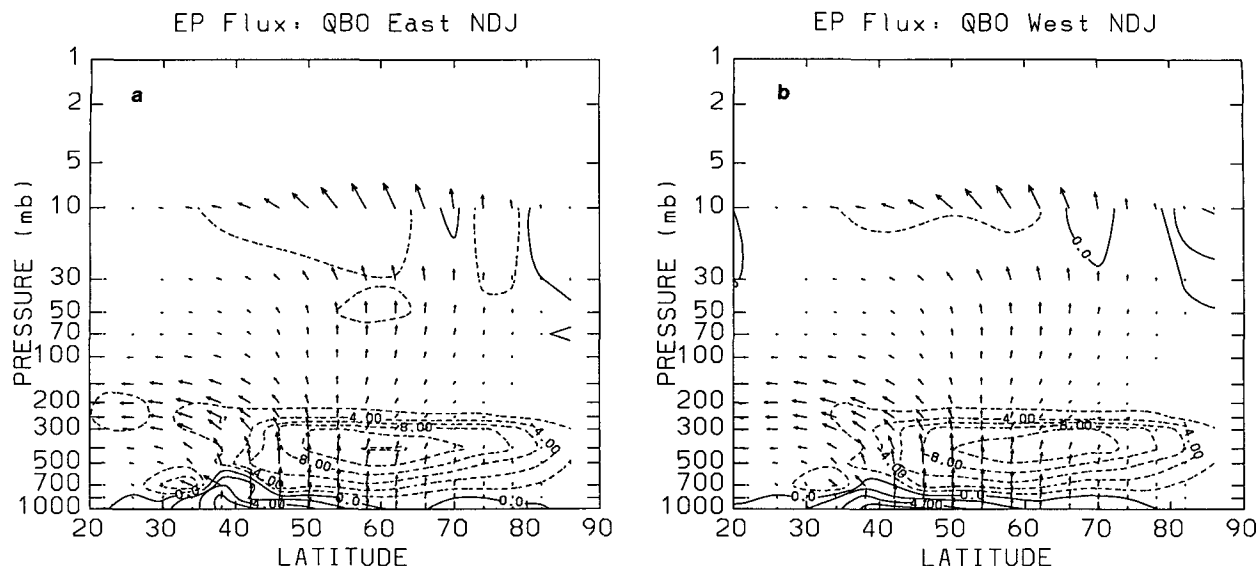


FIG. 15. NDJ Eliassen-Palm cross sections for (a) east category and (b) west category. Divergence contour interval is $2 \text{ m s}^{-1} \text{ day}^{-1}$, with negative values dashed.

to one-half of what would have been expected from the net flux alone. This suggests that the mean meridional circulation opposed the net flux and partially cancelled the effect of an imposed body force (Dunkerton et al. 1981; Garcia 1987; Dunkerton 1989). In both boxes, the net flux was due mainly to the vertical flux component entering the box from below.

The climatological 200- and 10-mb vertical flux is shown in Fig. 19, obtained from the 25-yr average. The average flux increases rapidly in early winter to a maximum in late December. Thereafter it declines slowly

until spring, with a slight local minimum in February. Note that the range of values was large (shown as average time series \pm one standard deviation).

c. QBO partitioning of integrated fluxes

Correlation of daily time series establishes that planetary-wave fluxes were closely tied to mean flow evolution in the northern winter stratosphere, especially above 10 mb. The obvious question is whether a *difference* in fluxes between the two QBO phase categories

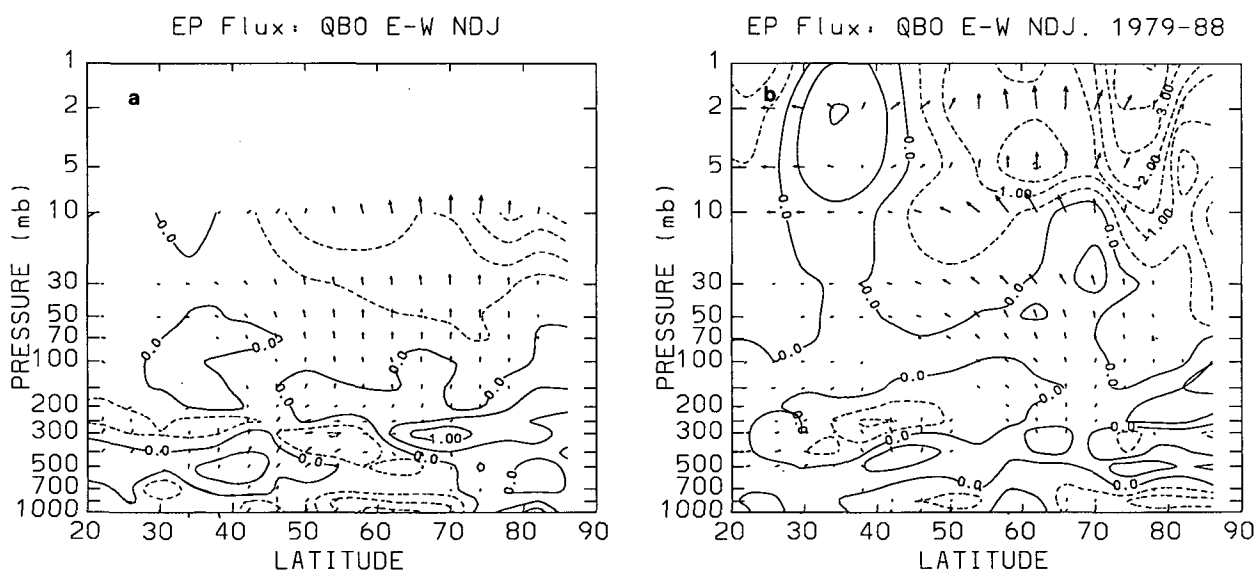


FIG. 16. Composite difference in NDJ Eliassen-Palm cross sections (east minus west) for (a) all years, (b) 1979-88 only. Divergence contour interval is $0.5 \text{ m s}^{-1} \text{ day}^{-1}$ with negative values dashed.

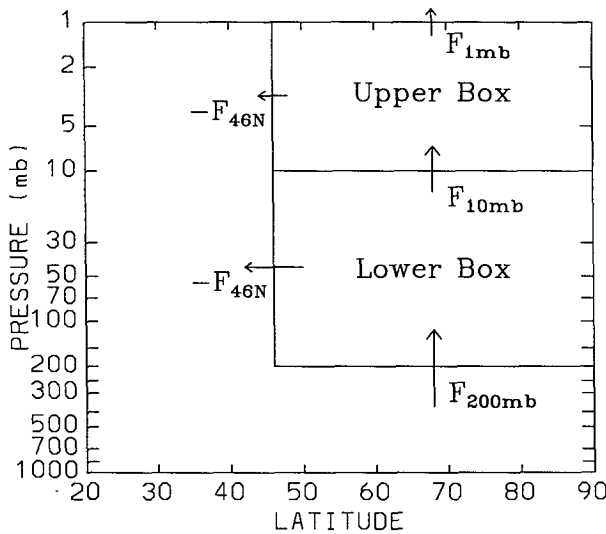


FIG. 17. Diagram of boxes used to calculate integrated fluxes and average angular momentum.

explained the interannual variation of mean circulation discovered by Holton and Tan (1980, 1982) and described in section 3 above. Composite differences shown in Fig. 16 supported this idea. Further evidence is presented in Fig. 20 where the climatological integrated fluxes of Fig. 19 were divided into east and west 40-mb QBO categories. In the east category, fluxes increased more rapidly in early winter and were smaller in late winter. For this reason the NDJ composite difference was slightly larger than DJF. The composite difference was small, however, in comparison to the total flux and its variation—as in the full cross section

of Fig. 16. To associate the flux difference with circulation anomalies it is necessary to establish a link between the net flux and angular momentum anomalies averaged over the appropriate time interval. From (5.3),

$$\langle M \rangle|_{t_1}^{t_2} + \dots = \int_{t_1}^{t_2} F_{\text{NET}} dt + \dots \quad (5.7)$$

Given the same initial conditions, a difference in early winter net flux should translate into a difference in midwinter angular momentum.

At this point, mixed results were found. For the lower box, the correlation between NDJ-averaged $\langle M \rangle$ and F_{NET} was 0.52 as shown in Fig. 21b. Major warmings were generally associated with anomalous convergence. In the upper box the same correlation for the last ten years was 0.62. This result seemed significant, even more so in the subtropical half of the dipole. There, in all five west (east) category years, the subtropical convergence was above (below) average. However, this result was obtained from only a 10-yr sample. (The calculation should be repeated in another decade.) In any case, something degraded the correlations between seasonally-averaged quantities, which were lower than the daily correlations discussed in connection with Fig. 18. It was probably the mean meridional circulation, noting the fact that the observed daily tendency was significantly lower than the daily flux convergence. The diabatic circulation persists even after an episode of wave activity ceases, further offsetting any induced change in mean circulation. Note that the observed QBO anomaly in the polar night jet was about 15 m s^{-1} , which would require a flux convergence difference of only about one-sixth of a meter per second per day—

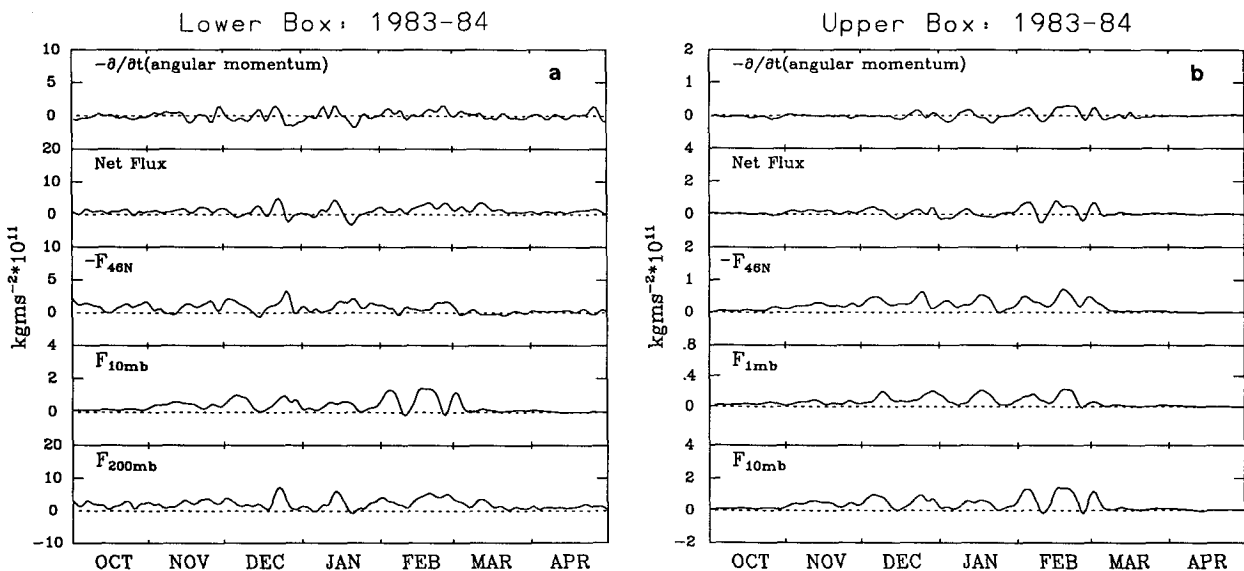


FIG. 18. Time series of box-integrated angular momentum tendency and flux components for 1983/84 winter. In this figure only, "net flux" represents convergence and the horizontal flux was inverted for clarity. See text for discussion. (a) Lower box; (b) upper box.

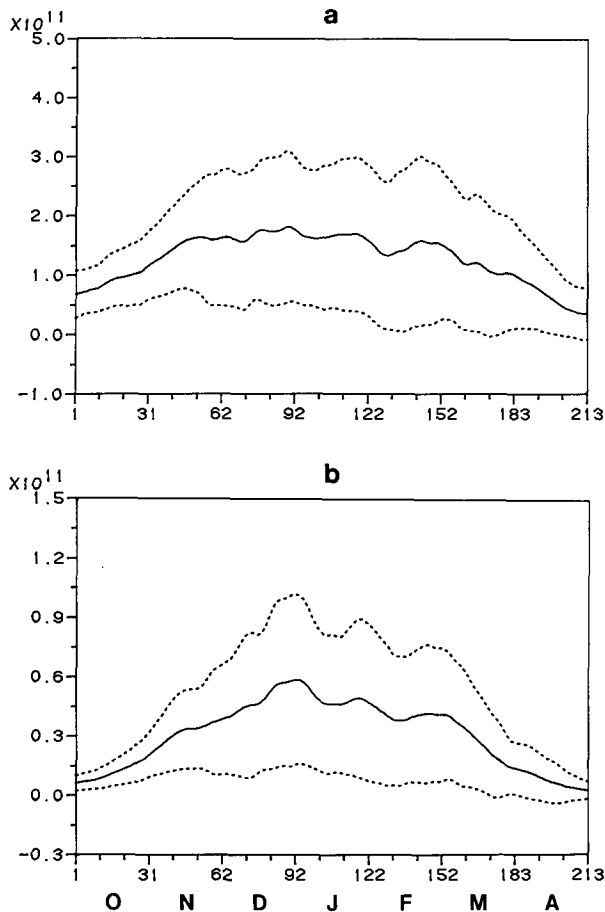


FIG. 19. Time series of climatological average (a) F_{200} , (b) F_{10} , the vertical components of integrated EP flux at 200 and 10 mb as defined in text. Average \pm one standard deviation shown as dashed lines. A 19-day running mean was used (Units: kg m s^{-2} .)

much less than the observed composite difference of Fig. 16 and a smaller ratio than that obtained from the daily data of Fig. 18.

d. Interpretation of the flux composite

Planetary-wave fluxes were evidently important in the extratropical oscillation. First, these fluxes were well correlated with mean circulation tendencies on a daily basis. Second, there was more flux convergence available than what was actually needed to cause observed mean flow tendencies. Some cancellation between body force and Coriolis torque probably occurred. Third, despite this cancellation it was possible to detect a difference in convergence and integrated fluxes between east and west QBO categories. In the east category, fluxes increased more rapidly in early winter and were reduced relative to the west category in late winter. To some extent this relationship held on a year-by-year basis.

From time series like those of Fig. 18 it is obvious that planetary fluxes varied considerably from week to week; sometimes the pulses were associated with major warmings, while at other times a sequence of 4 to 6 vacillation cycles was observed. The duration of pulses was commonly 2–3 weeks. Any differences in net flux between QBO east and west categories must be attributed to differences in events making up the composite. We attempted to determine whether there was any systematic difference between wave events in the two QBO categories. The question could be explained in this way:

- 1) whether there were more planetary wave events in the east category;
- 2) whether these events were larger in magnitude; and
- 3) whether the response of the mean flow was different in the two categories.

For this analysis, a wave “event” was defined as a 19-day interval centered about an amplification of R , where

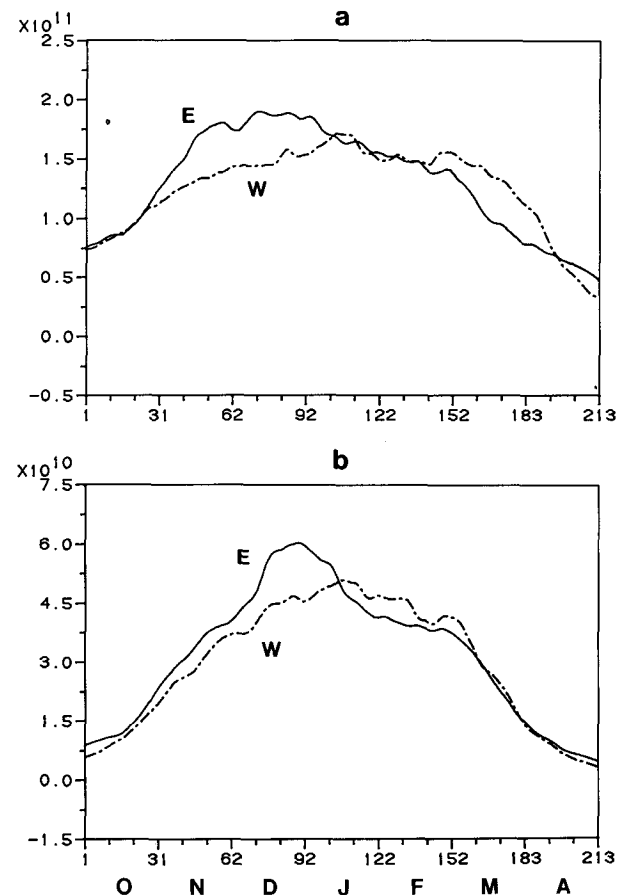


FIG. 20. Vertical EP flux as in Fig. 19 but for 40-mb east category (solid) and west category (dot-dash). (a) 200 mb; (b) 10 mb. A 31-day running mean was used to smooth sampling variations. (Units: kg m s^{-2} .)

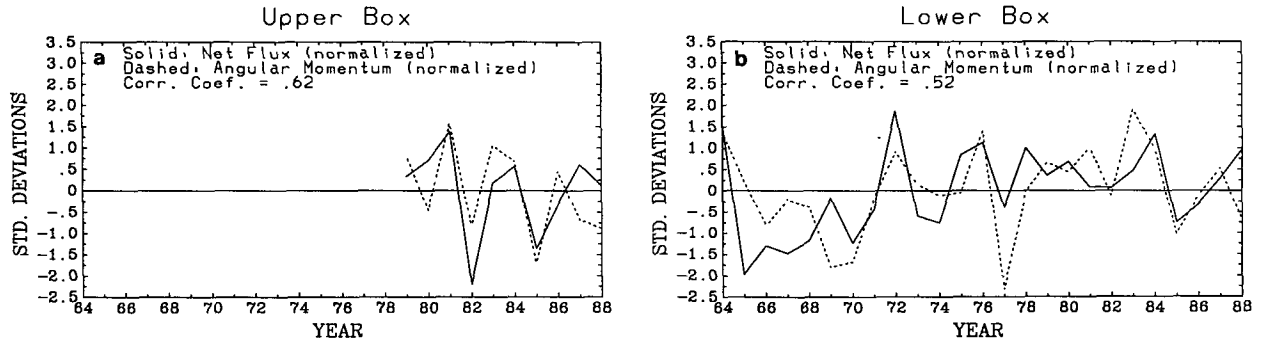


FIG. 21. Normalized NDJ net flux (solid) and angular momentum anomaly (dashed) for (a) upper box, (b) lower box.

$$R \equiv \sqrt{(F_{200}^*)^2 + (F_{10}^*)^2} \quad (5.8)$$

and

$$F_{10}^* \equiv F_{10}/\sigma_{10} \quad (5.9a)$$

$$F_{200}^* \equiv F_{200}/\sigma_{200} \quad (5.9b)$$

i.e., the integrated fluxes at 10 and 200 mb weighted by their respective standard deviation. The (arbitrary) criterion for an event was that R exceed 2.0. There were 105 such events in the 25-yr record. In NDJ, 36 occurred in the east category and 30 in the west category. A composite "life cycle" of integrated fluxes and $\langle M \rangle$ tendency for the lower box is shown in Fig. 22 for all events and for east and west categories separately. As one can see, differences between categories were generally small, the fluxes being only slightly larger in the east category. The difference in mean flow response

seemed more significant, particularly near the center day of the composite. In light of the fact that most of the flux dipole was located above 10 mb in Fig. 16b, we speculate that the different behavior of $\partial \langle M \rangle / \partial t$ may be due to a mean meridional circulation induced by fluxes above this level that were not observed prior to 1979.

Because of possible sampling errors one should not make too much of these differences. The overall structure of life cycle is probably more reliable, displaying a phase lag of 2–3 days between 200 and 10 mb, centered about day zero, and maximum net flux and mean flow response prior to the center day and slightly prior to the maximum in F_{200} . Relative to the maximum R at composite day 0, F_{200} and F_{10} maximize on day -1 and $+1$, respectively, while F_{NET} and angular momentum tendency maximize on day -2 . This timing is due to density weighting that favors the lower part of the box and to fluxes eventually escaping out of the top

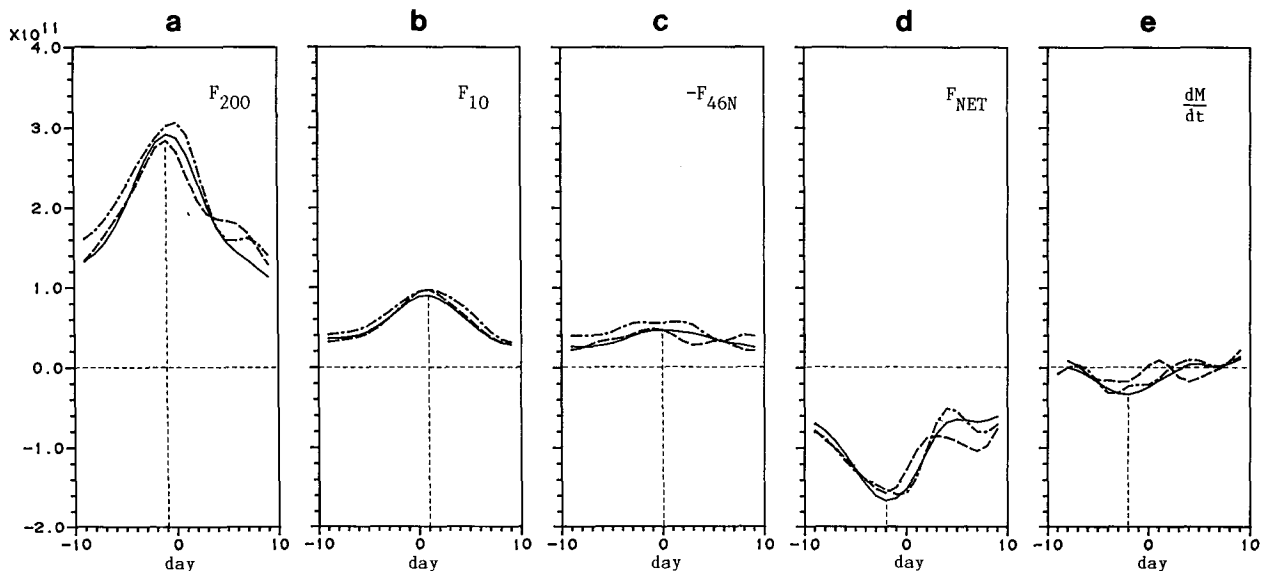


FIG. 22. Nineteen-day composite of planetary-wave life cycle using 105 events from all years (solid), 36 events from QBO east category (dot-dash), and 30 events from QBO west category (dashed). (a) F_{200} , (b) F_{10} , (c) $-F_{46N}$, (d) F_{NET} , and (e) $\partial \langle M \rangle / \partial t$. (Units: kg m s^{-2} .)

and side of the box, causing the net flux to begin decreasing in amplitude prior to day 0.

In summary, this analysis revealed only slight differences between east and west phase categories: slightly more events, slightly larger events, and a larger mean flow response in the east category. One should not overlook the fact that both categories had significant wave activity including major warmings. Also, in line with remarks made at the end of section 2, the evidence from planetary-wave fluxes added no *statistically independent information* to a proposed association between tropical and extratropical QBOs, because waves and mean flow were not independent in the extratropical stratosphere (as the day-to-day variability demonstrated).

We cannot state that planetary-wave fluxes were exclusively a "cause" of the extratropical QBO. Their effect was important, to be sure, but it is conceivable that *any other perturbation* to the mean flow could have its effect amplified by planetary-wave transport. This would occur whenever a positive feedback exists between wave-induced body force and mean flow deceleration.

6. Conclusion

Using 25 years of NMC data (1964–88), the relation between tropical and extratropical QBOs was examined for zonally averaged quantities (mean zonal wind, temperature, and geopotential) and quadratic wave quantities (Eliassen–Palm flux and its divergence). Our results added 11 years to an earlier study by Holton and Tan (1980, 1982) and confirmed that their extratropical oscillation existed in both temporal halves of the dataset. The apparent association between the two QBOs was strongest when the 40-mb equatorial wind was used. East phase at 40 mb implied a weaker than normal polar night jet and warmer than normal polar temperature and vice versa. The zonal wind anomaly was a dipole with approximately equal and opposite angular momentum in each half of the dipole. The association was most prominent between November and February, although the center of the dipole was observed to migrate poleward through the winter, possibly due to vortex erosion. The dipole was shown to be an important mode of interannual variability in the extratropical stratosphere, as suggested by earlier studies like van Loon et al. (1975) and Quiroz (1981), with possible influence extending into the troposphere. The mode might exist independently of the tropical QBO (because such high spatial autocorrelations were observed), but this idea leaves the extratropical oscillation unexplained, and significant correlation with tropical QBO. No attempt has been made here to separate other causes, such as ENSO; this issue and tropospheric interannual variability merit further investigation. The primary purpose of this paper has not been to establish a connection with the tropical QBO,

although one apparently exists, but to establish internal consistency between extratropical wave fluxes and mean circulation anomalies. This matter was left unresolved by Holton and Tan (1982). We have shown that there was very good daily correlation between Eliassen–Palm fluxes and observed angular momentum tendencies and that part of this correlation survived seasonal time-averaging, so that seasonally averaged fluxes displayed year-to-year variations fairly consistent with the zonally averaged oscillation. In other words, planetary-wave fluxes were an essential part of the extratropical QBO. Whether they were exclusively the cause of this QBO is uncertain, since any perturbation to the mean circulation could conceivably have its effect amplified by positive feedback due to wave–mean–flow interaction. Hopefully, this paper will motivate further theoretical and numerical study of these interactions and possible effects of the tropical QBO. Such an investigation could determine which upper or lower levels of the tropical QBO, if any, are responsible for observed changes in planetary-wave transport.

Acknowledgments. This research was supported by the National Science Foundation under Grants ATM-8616983, ATM-8819582, and ATM-9013280; by the National Aeronautics and Space Administration, Contracts NASW-4230 and NASW-4508; and by the National Oceanic and Atmospheric Administration, Grant NA90AA-D-AC807.

REFERENCES

- Andrews, D. G., J. R. Holton and C. B. Leovy, 1987: *Middle Atmosphere Dynamics*. Academic Press, 489 pp.
- Baldwin, M. P., and J. R. Holton, 1988: Climatology of the stratospheric polar vortex and planetary wave breaking. *J. Atmos. Sci.*, **45**, 1123–1142.
- , and T. J. Dunkerton, 1989a: Observations and statistical simulations of a proposed solar cycle/QBO/weather relationship. *Geophys. Res. Lett.*, **16**, 863–866.
- , and —, 1989b: The stratospheric major warming of early December 1987. *J. Atmos. Sci.*, **46**, 2863–2884.
- Bojkov, R. D., 1986: The 1979–1985 ozone decline in the Antarctic as reflected in ground based observations. *Geophys. Res. Lett.*, **13**, 1236–1239.
- Butchart, N., and E. E. Remsberg, 1986: The area of the stratospheric polar vortex as a diagnostic for tracer transport on an isentropic surface. *J. Atmos. Sci.*, **43**, 1319–1339.
- Dameris, M., and A. Ebel, 1990: The QBO and major stratospheric warmings: A three-dimensional model study. *Ann. Geophys.*, **8**, 79–86.
- Dole, R. M., 1983: Persistent anomalies of the extratropical Northern Hemisphere wintertime circulation. *Large-Scale Dynamical Processes in the Atmosphere*, B. Hoskins and R. Pearce, eds., Academic Press, 397 pp.
- Dunkerton, T. J., 1989: Body force circulations in a compressible atmosphere: Key concepts. *Pure Appl. Geophys.*, **130**, 243–262.
- , 1990: Annual variation of deseasonalized mean flow acceleration in the equatorial lower stratosphere. *J. Meteor. Soc. Japan*, **68**, 499–508.
- , C.-P. F. Hsu and M. E. McIntyre, 1981: Some Eulerian and Lagrangian diagnostics for a model stratospheric warming. *J. Atmos. Sci.*, **38**, 819–843.

- , and D. P. Delisi, 1985: Climatology of the equatorial lower stratosphere. *J. Atmos. Sci.*, **43**, 376–396.
- , and —, 1986: Evolution of potential vorticity in the winter stratosphere of January–February 1979. *J. Geophys. Res.*, **91**, 1199–1208.
- , —, and M. P. Baldwin, 1988: Distribution of major stratospheric warmings in relation to the quasi-biennial oscillation. *Geophys. Res. Lett.*, **15**, 136–139.
- Edmon, H. J., B. J. Hoskins and M. E. McIntyre, 1980: Eliassen–Palm cross sections for the troposphere. *J. Atmos. Sci.*, **37**, 2600–2616.
- Garcia, R. R., 1987: On the mean meridional circulation of the middle atmosphere. *J. Atmos. Sci.*, **44**, 3599–3609.
- , and S. Solomon, 1987: A possible relationship between interannual variability in Antarctic ozone and the quasi-biennial oscillation. *Geophys. Res. Lett.*, **14**, 848–851.
- Geller, M. A., 1989: Variations without forcing. *Nature*, **342**, 15–16.
- Hamilton, K., 1984: Mean wind evolution in the tropical lower stratosphere. *J. Atmos. Sci.*, **41**, 2113–2125.
- , 1990: A look at the recently proposed solar-QBO-weather relationship. *J. Clim.*, **3**, 497–503.
- Hitchman, M. H., C. B. Leovy, J. C. Gille and P. L. Bailey, 1987: Quasi-stationary zonally asymmetric circulations in the equatorial lower mesosphere. *J. Atmos. Sci.*, **44**, 2219–2236.
- Holton, J. R., 1983: The stratosphere and its links to the troposphere. *Large-Scale Dynamical Processes in the Atmosphere*, B. Hoskins and R. Pearce, eds., Academic Press, 397 pp.
- , and H.-C. Tan, 1980: The influences of the equatorial quasi-biennial oscillation on the global circulation at 50 mb. *J. Atmos. Sci.*, **37**, 2200–2208.
- , and —, 1982: The quasi-biennial oscillation in the Northern Hemisphere lower stratosphere. *J. Meteor. Soc. Japan*, **60**, 140–148.
- Kerr, R. A., 1989: Ozone hits bottom again. *Science*, **246**, 324.
- Killworth, P. D., and M. E. McIntyre, 1985: Do Rossby-wave critical layers absorb, reflect, or over-reflect? *J. Fluid Mech.*, **161**, 449–492.
- Labitzke, K., 1977: Interannual variability of the winter stratosphere in the Northern Hemisphere. *Mon. Wea. Rev.*, **105**, 762–770.
- , 1981: Stratospheric–mesospheric midwinter disturbances: A summary of observed characteristics. *J. Geophys. Res.*, **86**, 9665–9678.
- , 1982: On the interannual variability of the middle stratosphere during the northern winters. *J. Meteor. Soc. Japan*, **60**, 124–139.
- , 1987: Sunspots, the QBO, and the stratospheric temperature in the north polar region. *Geophys. Res. Lett.*, **14**, 535–537.
- , and H. van Loon, 1988: Associations between the 11-year solar cycle, the QBO, and the atmosphere. Part I: The troposphere and stratosphere in the Northern Hemisphere winter. *J. Atmos. Terr. Phys.*, **50**, 197–206.
- Lait, L. R., M. R. Schoeberl and P. A. Newman, 1989: Quasi-biennial modulation of the Antarctic ozone depletion. *J. Geophys. Res.*, **94**, 559–571.
- Livezey, R. E., and W. Y. Chen, 1983: Statistical field significance and its determination by Monte Carlo techniques. *Mon. Wea. Rev.*, **111**, 46–59.
- Matsuno, T., 1971: A dynamical model of the stratospheric sudden warming. *J. Atmos. Sci.*, **28**, 1479–1494.
- McIntyre, M. E., 1982: How well do we understand the dynamics of stratospheric warmings? *J. Meteor. Soc. Japan*, **60**, 37–65.
- , and T. N. Palmer, 1983: Breaking planetary waves in the stratosphere. *Nature*, **305**, 593–600.
- , and —, 1984: The “surf zone” in the stratosphere. *J. Atmos. Terr. Phys.*, **46**, 825–849.
- Naujokat, B., K. Labitzke, R. Lenschow, K. Petzoldt and R.-C. Wohlfart, 1988: The stratospheric winter 1987/88: An unusually early major midwinter warming. *Beil zur Berliner Wetterkarte*, **506**, 88.
- Quiroz, R. S., 1980: Variations in zonal mean and planetary wave properties of the stratosphere and links with the troposphere. *Pure Appl. Geophys.*, **118**, 416–427.
- , 1981: The tropospheric–stratospheric mean zonal flow in winter. *J. Geophys. Res.*, **86**, 7378–7384.
- , 1986: The association of stratospheric warmings with tropospheric blocking. *J. Geophys. Res.*, **91**, 5277–5285.
- Randel, W. J., 1987a: The evaluation of winds from geopotential height data in the stratosphere. *J. Atmos. Sci.*, **44**, 3097–3120.
- , 1987b: Global atmospheric circulation statistics, 1000–1 mb. NCAR Tech. Note. NCAR/TN-295+STR, 245 pp.
- Robinson, W., 1986: The application of the quasi-geostrophic Eliassen–Palm flux to the analysis of stratospheric data. *J. Atmos. Sci.*, **43**, 1017–1023.
- Scherhag, R., 1952: Die explosionsartigen Stratosphärenwärmungen des Spät winters 1951–1952. *Ber. Deut. Wetterd.*, **6**, 51–63.
- Schoeberl, M. R., 1978: Stratospheric warmings: Observations and theory. *Rev. Geophys. Space Phys.*, **16**, 521–538.
- Trenberth, K. E., 1980: Atmospheric quasi-biennial oscillations. *Mon. Wea. Rev.*, **108**, 1370–1377.
- van Loon, H., R. A. Madden and R. L. Jenne, 1975: Oscillations in the winter stratosphere: Part 1: Description. *Mon. Wea. Rev.*, **103**, 154–162.
- , C. S. Zerefos and C. C. Repapis, 1982: The southern oscillation in the stratosphere. *Mon. Wea. Rev.*, **110**, 225–229.
- , and K. Labitzke, 1987: The southern oscillation. Part V: The anomalies in the lower stratosphere of the Northern Hemisphere in winter and a comparison with the quasi-biennial oscillation. *Mon. Wea. Rev.*, **115**, 357–369.
- Wallace, J. M., and D. S. Gutzler, 1981: Teleconnections in the geopotential height field during the northern winter. *Mon. Wea. Rev.*, **109**, 784–812.
- , and F.-C. Chang, 1982: Interannual variability of the wintertime polar vortex in the Northern Hemisphere middle stratosphere. *J. Meteor. Soc. Japan*, **60**, 149–155.